Antioxidant activity and interaction with DNA and albumins of zinc–tolfenamato complexes. Crystal structure of [Zn(tolfenamato)2(2,2′-dipyridylketoneoxime)2]

ARTICLE *in* EUROPEAN JOURNAL OF MEDICINAL CHEMISTRY · JANUARY 2014

Impact Factor: 3.45 · DOI: 10.1016/j.ejmech.2013.12.019 · Source: PubMed

7 AUTHORS, INCLUDING:

Jakob Kljun
Faculty of Chemistry and Chemical Technol…
22 PUBLICATIONS **332** CITATIONS
SEE PROFILE

Dimitris P Kessissoglou
Aristotle University of Thessaloniki
94 PUBLICATIONS **3,347** CITATIONS
SEE PROFILE

European Journal of Medicinal Chemistry 74 (2014) 187–198

Contents lists available at ScienceDirect

European Journal of Medicinal Chemistry

journal homepage: http://www.elsevier.com/locate/ejmech

Original article

Antioxidant activity and interaction with DNA and albumins of zinc–tolfenamato complexes. Crystal structure of [Zn(tolfenamato)$_2$(2,2′-dipyridylketoneoxime)$_2$]

Alketa Tarushi [a], Xanthippi Totta [a], Athanasios Papadopoulos [b], Jakob Kljun [c,d], Iztok Turel [d], Dimitris P. Kessissoglou [a], George Psomas [a,*]

[a] Laboratory of Inorganic Chemistry, Department of General and Inorganic Chemistry, Faculty of Chemistry, Aristotle University of Thessaloniki, GR-54124 Thessaloniki, Greece
[b] Department of Nutrition and Dietetics, Faculty of Food Technology and Nutrition, Alexandrion Technological Educational Institution, Sindos, Thessaloniki, Greece
[c] EN-FIST Centre of Excellence, Dunajska 156, 1000 Ljubljana, Slovenia
[d] Faculty of Chemistry and Chemical Technology, University of Ljubljana, Askerceva 5, 1000 Ljubljana, Slovenia

ARTICLE INFO

Article history:
Received 5 November 2013
Received in revised form
20 December 2013
Accepted 21 December 2013
Available online 3 January 2014

Keywords:
Zinc(II) complexes
Tolfenamic acid
Interaction with calf-thymus DNA
Interaction with serum albumins
Antioxidant activity

ABSTRACT

The zinc(II) complex of the non-steroidal anti-inflammatory drug tolfenamic acid (=Htolf) in the presence of 2,2′-dipyridylketone oxime (=Hpko) as a *N*,*N*′-donor heterocyclic ligand, [Zn(tolf-O)$_2$(Hpko-*N*,*N*′)$_2$]·MeOH (=**1**·MeOH), has been synthesized and characterized by physicochemical techniques including X-ray crystallography. The complex exhibits good binding affinity to human or bovine serum albumin with high binding constant values. Complex **1** and previously reported Zn-tolfenamato complexes were tested for their free radical scavenging activity and *in vitro* inhibitory activity against soybean lipoxygenase and exhibited significant activity with [Zn(tolf)$_2$(1,10-phenantroline)] being the most active compound. The complexes interact with calf-thymus (CT) DNA via intercalation, and can displace the DNA-bound ethidium bromide with **1** exhibiting the highest binding constant to CT DNA.

1. Introduction

Zinc is the second most abundant trace element in the human body, has a major regulatory role in the metabolism of cells [1] and presents many beneficial effects to human health, while changes in its metabolism or trafficking are related to some diseases [2,3]. Zinc is extensively used to treat children suffering from deadly diarrhea resulting in significant reduction of child mortality in many countries of Asia and Africa [4]. The role of zinc in nucleic acid chemistry is noteworthy since zinc(II) ions are the only metal ions able to facilitate the rewinding of molten DNA [5]. In the literature diverse zinc compounds have exhibited a potential biological activity with zinc complexes with drugs being tested for the treatment of Alzheimer disease [6] and others showing antibacterial [7,8], anticonvulsant [9], antidiabetic [10], anti-inflammatory [11], antioxidant [12] and antiproliferative-antitumor [8,11] activity.

Non-steroidal anti-inflammatory drugs (NSAIDs)[†] are among the most frequently used drugs as analgesics, anti-inflammatories and antipyretics with known side-effects (mainly gastrointestinal such as gastric ulceration, nausea, diarrhea and renal including salt and fluid retention, hypertension, and in rare cases interstitial nephritis, acute renal failure) [13]. The inhibition of the cyclo-oxygenase (COX)-mediated production of prostaglandins is the main mode of action of the NSAIDs [14]. They have also shown a synergistic role on the activity of certain antitumor drugs [15] and have presented antitumor activity leading to cell death of a series of cancer cell lines via apoptotic pathways [16] or via diverse molecular

Abbreviations: ABTS, 2,2′-azinobis-(3-ethylbenzothiazoline-6-sulfonic acid) radical cation; BHT, butylated hydroxytoluene; bipy, 2,2′-bipyridine; BSA, bovine serum albumin; COX, cyclo-oxygenase; CT, calf-thymus; DMF, *N*,*N*-dimethylformamide; DMSO, dimethylsulfoxide; DPPH, 1,1-diphenyl-picrylhydrazyl; EB, ethidium bromide, 3,8-diamino-5-ethyl-6-phenyl-phenanthridinium bromide; Hpko, 2,2′-dipyridylketone oxime; Htolf, tolfenamic acid, 2-[(3-chloro-2-methylphenyl)amino]benzoic acid; HSA, human serum albumin; LOX, soybean lipoxygenase; NDGA, nordihydroguaiaretic acid; NSAID, non-steroidal anti-inflammatory drug; phen, 1,10-phenanthroline; RA, DPPH radical scavenging activity; SA, serum albumin; tolf, tolfenamato, anion of tolfenamic acid.

* Corresponding author. Tel.: +30 2310997790; fax: +30 2310997738.
E-mail address: gepsomas@chem.auth.gr (G. Psomas).

0223-5234/$ – see front matter © 2013 Elsevier Masson SAS. All rights reserved.
http://dx.doi.org/10.1016/j.ejmech.2013.12.019

mechanisms [17] where free radicals have been also involved [18]. In an attempt to investigate potential mechanisms of the anticancer as well as the anti-inflammatory activity of the NSAIDs and their complexes, the interaction with DNA as well as the antioxidant activity are considered of great importance and should be further evaluated; it is noteworthy that only few relevant reports on the interaction of NSAIDs and their complexes with DNA have been published so far [19,20]. Furthermore, the number of structurally characterized zinc complexes with NSAIDs [21] is still expanding including an aspirinate complex [22], a flufenamato complex [23] and a series of complexes with indomethacin [8], mefenamic acid [12] and tolfenamic acid [24] as ligands.

Tolfenamic acid (=Htolf, Scheme 1) is a NSAID belonging to the *N*-phenylanthranilic acid derivatives with similar properties to mefenamic acid and flufenamic acid and other fenamates in clinical use [25]. Htolf is found in diverse analgesic, anti-inflammatory, antipyretic and antirheumatoid drugs and is also used for veterinary purposes [26]. The crystal structures of a series of tin(IV) [27], copper(II) [28,29], cobalt(II) [30], and zinc(II) [24] complexes with tolfenamato ligands have been reported in the literature.

Taking into consideration the significance of NSAIDs in medicine and the presence of zinc in diverse drugs, we have synthesized and characterized the structure and the spectroscopic (IR, UV and ^{1}H NMR) properties of the neutral zinc(II) complexes with the NSAID tolfenamic acid in the presence of the *N*,*N*′-donor heterocyclic ligand 2,2′-dipyridylketone oxime (=Hpko). The crystal structure of the resultant complex [Zn(tolf-O)$_2$(Hpko-*N*,*N*′)$_2$]·MeOH, **1**·MeOH has been determined by X-ray crystallography. Furthermore, the ^{1}H NMR spectra of the recently reported Zn-tolfenamato complexes [Zn(tolf)(phen)Cl] (**2**), [Zn(tolf)(bipy)Cl], (**3**), [Zn(tolf)$_2$(phen)], (**4**), [Zn(tolf)$_2$(bipy)], (**5**) and [Zn$_3$(tolf)$_6$(MeOH)$_2$] (**6**) (where phen and bipy are the *N*,*N*′-donor heterocyclic ligands 1,10-phenanthroline and 2,2′-bipyridine, respectively) [24] have been recorded and evaluated. In an attempt to further investigate the existence of potential anti-inflammatory activity of complexes **1**–**6**, the study of their biological properties has been focused on (i) their antioxidant capacity by investigating their scavenging ability of 1,1-diphenyl-picrylhydrazyl (DPPH) and 2,2′-azinobis-(3-ethylbenzothiazoline-6-sulfonic acid) (ABTS$^{+\bullet}$) radicals, their ability to antagonize DMSO in hydroxyl radicals ($^\bullet$OH) binding, as well as their *in vitro* inhibitory activity against soybean lipoxygenase (LOX), because the use of NSAIDs in medicine as anti-inflammatories is also related to free radicals scavenging, (ii) the affinity of the complexes to bovine (BSA) and human serum albumin (HSA), as characteristic serum proteins, investigated by fluorescence spectroscopy since the binding to these proteins which are involved in the transport of metal ions and metal-drug complexes through the blood stream may result in lower or enhanced biological properties of the original drug, or may propose new paths for drug transportation [31], (iii) their binding properties with calf-thymus (CT) DNA investigated by UV spectroscopy and viscosity measurements and ethidium bromide (EB) displacement ability from the EB-DNA compound performed by fluorescence spectroscopy (EB is a typical DNA-intercalator and the competition with it for the DNA intercalation sites may serve as an indirect evidence of potential intercalation).

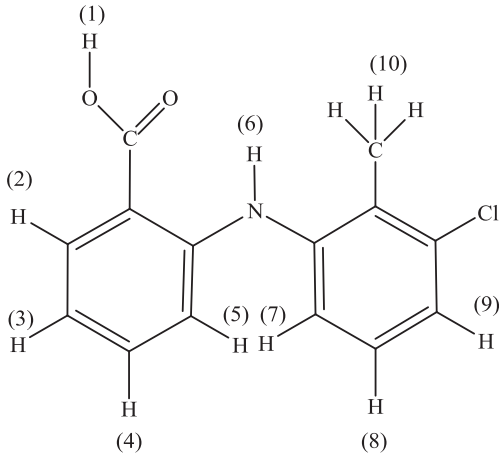

Scheme 1. Tolfenamic acid (=Htolf) with H atom numbering in accordance to ^{1}H NMR proton's assignment.

2. Results and discussion

2.1. Synthesis and spectroscopic characterization

The synthesis of complex **1** was achieved in high yield via the aerobic reaction of tolfenamic acid, deprotonated by KOH, with $ZnCl_2$ in the presence of the *N*,*N*′-donor heterocyclic ligand Hpko in a ratio Zn^{2+}:tolf$^-$:Hpko of 1:2:2. The complex is stable in air, soluble in DMSO and DMF and non-electrolyte in DMSO (for 1 mM solution, 15 μS/cm). Complex **1** was characterized by elemental analysis, IR, UV and ^{1}H NMR spectroscopic techniques and by X-ray crystallography. Additionally, the ^{1}H NMR spectra of compounds **2**–**6** were recorded and evaluated.

IR spectroscopy is a useful tool to confirm the deprotonation and the binding mode of tolfenamic acid. In the IR spectrum of Htolf, the absorption band at 3355(br,m) cm^{-1}, attributed to the ν(H–O) stretching vibration has disappeared upon binding to the zinc ion. The strong bands appearing at 1661 cm^{-1} and 1265 cm^{-1} which were attributed to ν(C=O)$_{carboxylic}$ and ν(C–O)$_{carboxylic}$ stretching vibrations of the carboxylic moiety (-COOH) of Htolf, respectively, have shifted, in the IR spectra of complex **1**, at 1584 cm^{-1} and 1387 cm^{-1} assigned to antisymmetric, ν_{asym}(C=O), and symmetric, ν_{sym}(C=O), stretching vibrations of the coordinated carboxylato group, respectively. The parameter Δ [=ν_{asym}(C=O) − ν_{sym}(C=O)] which is a useful characteristic tool for determining the coordination mode of the carboxylato ligands, has a value of 197 cm^{-1} that is indicative of asymmetrically monodentate binding mode of the tolfenamato ligands [24,30].

^{1}H NMR spectroscopy can be considered a valuable tool to study the behavior of complexes in solution. The recorded ^{1}H NMR spectra of compounds **1**–**6** in DMSO-d_6 solution confirm the formulae and the purity of the prepared compounds as well as the integrity of each complex in solution. More specifically, in the ^{1}H NMR spectra of complexes **1**–**6**, the absence of the signal at 13.10 ppm assigned to carboxylic hydrogen of the free tolfenamic acid [32] confirms the deprotonated mode of the bound drug, while the rest signals of the tolfenamato ligand are slightly shifted downfield or upfield as expected upon binding to zinc metal ion [12,23,33,34]. Furthermore, all sets of signals related to the presence of the *N*-donor ligands are present and the ratios of integrated peaks confirm the ratio of ligands in the solid state, e.g. representatively for **1**, **2** and **4** in Fig. 1: (i) four signals for bipy or phen ligands and (ii) seven signals for Hpko ligands; six of them are attributed to aromatic hydrogen atoms and the seventh signal at 12.21 ppm is assigned to the oxime hydroxyl proton confirming that the Hpko ligand is bound in its non-deprotonated state. The absence of any additional sets of signals related to dissociated ligands is in agreement with the molecular conductance measurements and suggests that all complexes remain intact in solution [35–37].

The UV–vis spectra of complex **1** were recorded as nujol mull and in DMSO solution and were similar suggesting that it retains its structure in solution. Additionally, in order to explore the stability

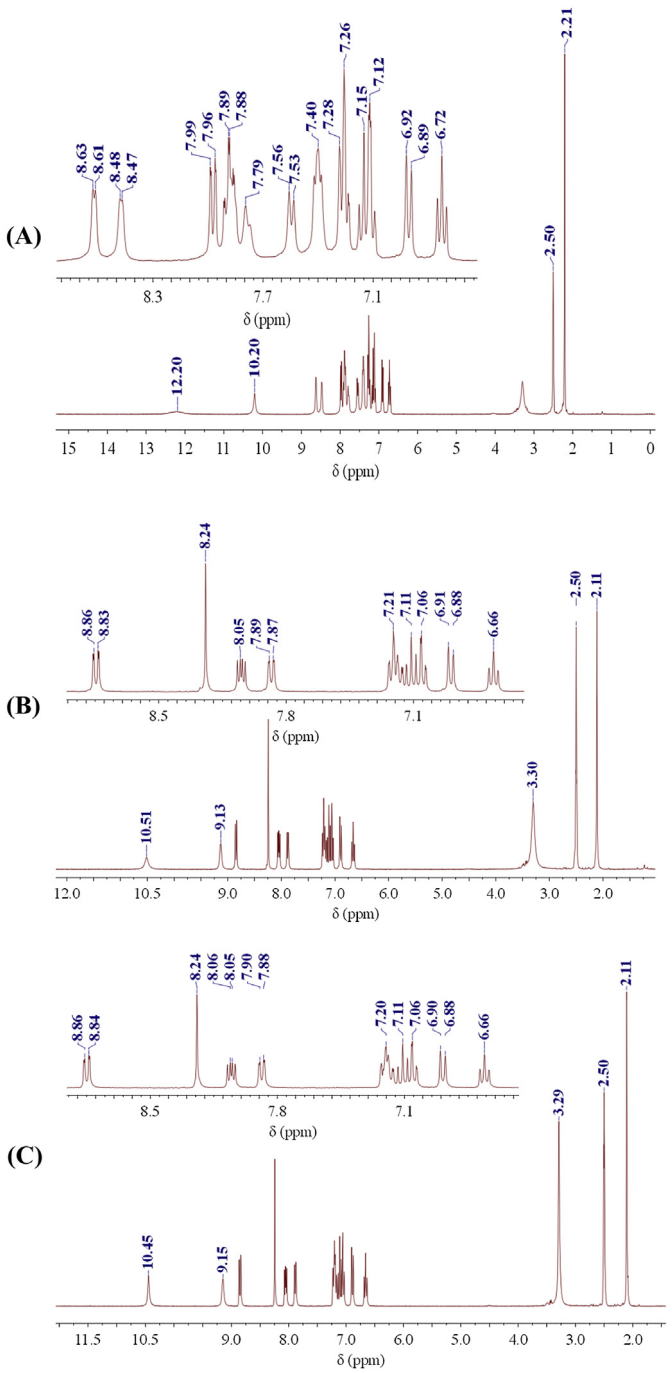

Fig. 1. ^{1}H NMR spectra of (A) **1**, (B) **2** and (A) **4** in DMSO-d_6.

of the complex in buffer solution, the UV–Vis spectra in the series of pH (pH range 6–8, since the biological experiments are performed at pH = 7) with the use of diverse buffer solutions (150 mM NaCl and 15 mM trisodium citrate at pH values regulated by HCl solution) have also been recorded. No significant changes (shift of the λ_{max} or new peaks) have been observed indicating that the complex keeps its integrity in the pH range 6–8. The same behavior in solution has been reported for complexes **2**–**6** [24].

The fluorescence emission spectra of the complexes have been recorded in DMSO solution. As an example, the fluorescence excitation and emission spectra for complexes **1** and **4** are shown in Fig. 2. When all complexes are excited in the range of $\lambda_{ex,max}$ 370–390 nm, they exhibit an intense emission band with $\lambda_{em,max}$ lying in the region 438–445 nm and a second band (as a peak or as a shoulder) of lower intensity at 483–488 nm. An additional pair of excitation and emission bands at 330 nm and 395 nm, respectively, has been observed for complex **3** (Table S1).

The fact that the complexes are non-electrolytes in DMSO solution ($\Lambda_M \leq 15$ μS/cm, in 1 mM DMSO solution), they have the same UV–Vis spectral pattern in nujol and in DMSO solution, as well as in buffer solution, and all ^{1}H NMR spectra confirm that the complexes do not dissociate, suggests that the compounds are stable and keep their integrity in solution. We have reported earlier that Co(II) tolfenamato complexes [30] as well as the Zn(II) mefenamato complexes [12] are also stable in solution.

2.2. Structure of *cis, cis, trans*-[Zn(tolf-*O*)$_2$(Hpko-*N*,*N*′)$_2$]·CH_3OH, 1·CH_3OH

A drawing of the molecular structure of [Zn(tolf-*O*)$_2$(Hpko-*N*,*N*′)$_2$], **1** is shown in Fig. 3 and selected bond distances and angles are listed in Table 1.

In complex **1**, the zinc atom is six-coordinate surrounded by two tolfenamato ligands and two Hpko showing a distorted octahedral environment with a ZnN_4O_2 metal center. The bond distances around Zn atom are not equal (Table 1) with Zn–O bond distances (Zn(1)–O(8) = 2.0384(14) Å and Zn(1)–O(9) = 2.0768(13) Å) being shorter than the Zn–N bond distances (Zn(1)–N(10) = 2.1748(17) Å, Zn(1)–N(14) = 2.1602(16) Å, Zn(1)–N(15) = 2.1777(16) Å and Zn(1)–N(17) = 2.1316(17) Å). These distances are consistent with those of previously reported structurally related zinc complexes with fenamic acid NSAIDs and bidentate nitrogen ligands, [Zn(tolf)$_2$(bipy)], [Zn(tolf)$_2$(phen)] [24], [Zn(mefenamato)$_2$(bipy)], [Zn(mefenamato)$_2$(bipyam)], [Zn(mefenamato)$_2$(phen)(H_2O)] [12], [Zn(bipy)$_2$(ONO)](NO_2) [38], [Zn(phen)$_2$($MeCO_2$)](ClO_4) [39], and [Zn(pipdtc)$_2$(bipy)] (pipdtc$^-$ = piperidine–carbodithioato anion) [40] and is isostructural with its mefenamato analogue *cis*,*cis*,*trans*-[Zn(mefenamato-*O*)$_2$(Hpko-*N*,*N*′)$_2$]·EtOH recently published by our group [12].

The tolfenamato ligands behave as deprotonated monodentate ligands coordinated to zinc ion via a carboxylato-oxygen atom. The carboxylate groups of the tolfenamato ligands are monodentately bound to zinc in asymmetric fashion (C(56)–O(6) = 1.265(2) Å and C(56)–O(9) = 1.273(2) Å, C(52)–O(7) = 1.260(2) Å and C(52)–O(8) = 1.274(2) Å). Weak intraligand interactions through hydrogen bonds between the amine hydrogen atoms and the coordinated oxygen atoms (H(12)···O(8) = 1.961 Å and H(13)···O(9) = 2.016 Å) contribute to the stabilization of the complex (Table S2).

The Hpko ligands act as bidentate neutral chelators and are coordinated to zinc via one pyridine nitrogen and the oxime nitrogen with the ketonoxime oxygen remaining unbound. This coordination mode of Hpko ligand (1.0110 according to the Harris notation [41]) has been observed in a series of mononuclear metal complexes [42], [Zn(mefenamato)$_2$(Hpko)$_2$] [12] and in the trinuclear Ni(II) complex [Ni_3(shi)$_2$(Hpko)$_2$(py)$_2$] (where H_3shi = salicylhydroxamic acid and py = pyridine) [43]. The ketoxime groups also form hydrogen bonds with the uncoordinated carboxylic oxygens of the adjacent tolfenamato ligands (H(5)···O(6) 1.706 Å and H(4)···O(7) 1.709 Å; Table S2). The lattice is further stabilized by the formation of a hydrogen bond between the solvate methanol molecule and one of the uncoordinated pyridine nitrogen atoms of a dipyridylketoxime ligand (N(18)).

2.3. Antioxidant capacity of the compounds

It is known that free radicals play an important role in the inflammatory process. Compounds with antioxidant properties could

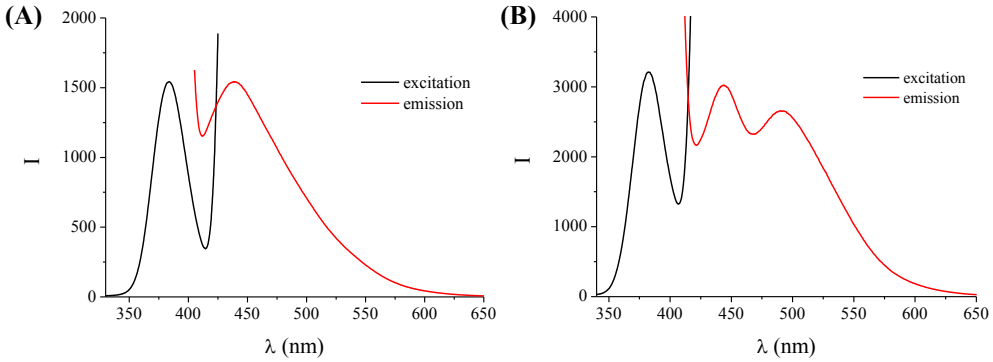

Fig. 2. Fluorescence spectra (emission in red, excitation in black) of complex (A) **1** (λ_{ex} = 390 nm, λ_{em} = 438 nm) and (B) **4** (λ_{ex} = 384 nm, λ_{em} = 438 and 488 nm) in DMSO solution. (For interpretation of the references to colour in this figure legend, the reader is referred to the web version of this article.)

potentially have a crucial role against inflammation and, thus, lead to potentially effective drugs. NSAIDs are drugs capable to act either as inhibitors of free radical production or as radical scavengers [44] and the antioxidant activity shown by NSAIDs and their complexes could be considered as first evidence of a potential anticancer and anti-inflammatory activity. Therefore, the potential antioxidant ability of complexes **1**–**6** has been evaluated in regard to DPPH, ABTS and hydroxyl radical scavenging ability as well as the *in vitro* soybean lipoxygenase inhibition and has been compared to that of well-known antioxidant agents (e.g. nordihydroguaiaretic acid (NDGA), butylated hydroxytoluene (BHT), 6-hydroxy-2,5,7,8-tetramethylchromane-2-carboxylic acid (trolox) and caffeic acid) used as reference compounds.

Compounds that can scavenge DPPH radicals also present anti-ageing, anticancer and anti-inflammatory activity [45]. Therefore, the compounds exhibiting DPPH radical scavenging activity are of increasing interest because of their potential protection against rheumatoid arthritis and inflammation which may lead to potentially effective drugs. DPPH is a stable free radical presenting a strong absorption band at 517 nm, which decreases, when antioxidants donate protons to DPPH radical. The scavenging activity of almost all complexes with exception of **5** and **6** was time-independent since no significant changes were observed after 20-min and 60-min measurements (Table S3). The complexes present low to moderate reducing ability of DPPH radical compared to the reference compound NDGA while their DPPH scavenging activity is similar to BHT. All complexes but **3** show higher DPPH radical scavenging activity than free tolfenamic acid with [Zn(tolf)$_2$(phen)] being the best DPPH scavenger (Fig. 4(A)) among complexes **1**–**6**. The complexes present similar scavenging activity of the DPPH radical to that found for a series of zinc(II), copper(II) and cobalt(II) complexes with mefenamic acid as ligand [12,46,47].

Hydroxyl radicals are among the most reactive oxygen species. Compounds capable to act as hydroxyl radical scavengers may also serve as protectors activating the prostaglandin synthesis since the superoxide anion radicals are generated by phagocytes at the inflamed site during the inflammatory process and are connected to other oxidizing species such as •OH [46]. Complexes **1**–**6** exhibit higher competition with DMSO (33 mM) at 0.1 mM for hydroxyl free radicals than free tolfenamic acid and the reference compound trolox (Table S4) with complex **6** being the most active compound (•OH% = 96.40(±0.57) %) and complexes **1** and **3** presenting similar hydroxyl scavenging ability (Fig. 4(B)). The hydroxyl radical scavenging actility of complexes **1**–**6** is of the same magnitude to that found for zinc(II), copper(II), and cobalt(II) mefenamato complexes [12,46,47].

The ability of the compounds to scavenge the cationic radical of ABTS (ABTS^{+}•) is related to the magnitude of the total antioxidant activity of the compounds [46]. Complexes **1**–**6** show significant ABTS radical scavenging activity which is higher than free Htolf, but lower than that of the reference compound trolox except complex **4** which is the most active ABTS scavenger among the complexes (ABTS% = 93.62(±0.75)%) and even more active than trolox (Table S4). The results are in agreement to DPPH and hydroxyl

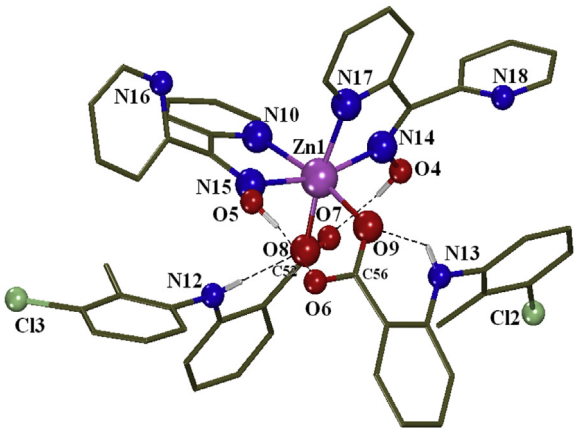

Fig. 3. A drawing of the molecular structure of **1** with only the heteroatoms labeling.

Table 1
Selected bond distances and angles for complex **1**.

Bond	Distance (Å)	Bond	Distance (Å)
Zn(1)–O(8)	2.0384(14)	Zn(1)–N(14)	2.1602(16)
Zn(1)–O(9)	2.0768(13)	Zn(1)–N(17)	2.1316(17)
Zn(1)–N(10)	2.1748(17)	Zn(1)–N(15)	2.1777(16)
O(6)–C(56)	1.265(2)	O(7)–C(52)	1.260(2)
O(9)–C(56)	1.273(2)	O(8)–C(52)	1.274(2)
O(4)–N(14)	1.367(2)	O(5)–N(15)	1.370(2)
Bond angle	**(°)**	**Bond angle**	**(°)**
O(8)–Zn(1)–O(9)	85.57(6)	O(9)–Zn(1)–N(10)	169.76(6)
O(8)–Zn(1)–N(10)	89.84(6)	O(9)–Zn(1)–N(14)	94.04(6)
O(8)–Zn(1)–N(14)	97.38(6)	O(9)–Zn(1)–N(15)	96.41(6)
O(8)–Zn(1)–N(15)	95.23(6)	O(9)–Zn(1)–N(17)	89.17(6)
O(8)–Zn(1)–N(17)	171.05(6)	N(14)–Zn(1)–N(15)	164.19(6)
N(10)–Zn(1)–N(14)	95.62(6)	N(14)–Zn(1)–N(17)	75.75(6)
N(10)–Zn(1)–N(15)	74.88(6)	N(15)–Zn(1)–N(17)	92.54(6)
N(10)–Zn(1)–N(17)	96.47(6)		

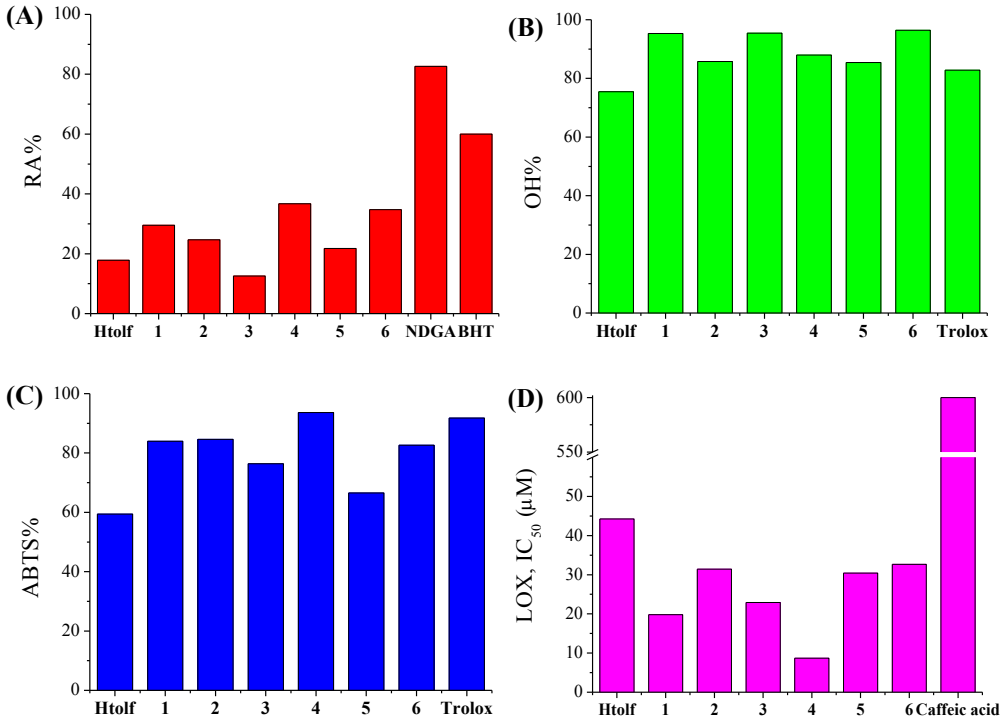

Fig. 4. (A) Interaction % with DPPH (RA%), (B) competition% with DMSO for hydroxyl radical (•OH%), (C) % superoxide radical scavenging activity (ABTS%) and (D) *in vitro* inhibition of soybean lipoxygenase (LOX) (IC_{50}, in μM) for Htolf and complexes **1**–**6**.

radical scavenging studies with the complexes being more active scavengers than free Htolf (Fig. 4(C)(C)). Similar scavenging activity of the ABTS radical has been recorded for Zn(II), Cu(II), and Co(II) mefenamato complexes [12,46,47].

Lipoxygenases (LOXs) are a family of non-heme iron-containing dioxygenases and are the key enzymes of the transformation of arachidonic acid to leukotrienes, compounds playing an important role in the pathophysiology of several inflammatory and allergic diseases. The products of the oxygenation catalysed by LOXs are also involved in the development of rheumatoid arthritis, psoriasis and asthmatic responses [12]. Most LOX inhibitors could be considered as potential antioxidants or free radical scavengers since lipoxygenation occurs via a carbon centered radical [48]. The "non-heme" iron per molecule of LOXs in the enzyme active site is a high-spin Fe(III) in the activated state and a high-spin Fe(II) in the inactive state. The ability of LOX inhibitors, which are considered excellent ligands for Fe(III), to reduce the Fe(III) at the active site to the catalytically inactive Fe(II) has been closely related to LOX inhibition [49].All complexes present significant inhibition against soybean lipoxygenase (Table S4), especially in relation to the reference compound caffeic acid (IC_{50} = 600 μM). The complexes present slightly better LOX inhibition activity than free Htolf and **4** is the most active compound against LOX (IC_{50} = 8.71(±0.76) μM) (Fig. 4(D)).

In conclusion, the complexes exhibit higher radical scavenging and LOX inhibitory activity than free tolfenamic acid with complex 4 considered the most active scavenger among the complexes examined. A series of Cu(II), Co(II), Ni(II), Zn(II), and Pd(II) complexes with diverse ligands exhibiting enhanced antioxidant activity in comparison to corresponding free ligands have been found in the literature [12,45,46,50–54]. In general all complexes present low to moderate activity against DPPH and high activity against hydroxyl and ABTS radicals, a fact that could be considered evidence of selective scavenging activity of the complexes against hydroxyl and ABTS radicals. In the literature, there are examples of complexes being more active against DPPH radicals than •OH or $ABTS^{+\bullet}$ [55,56] and others with zinc complexes among them exhibiting much more significant hydroxyl and ABTS scavenging activity than DPPH [50–54,57,58]. The zinc–tolfenamato complexes **1**–**6** exhibit similar or better free radical scavenging activity (RA% = 12.5–36.7%, •OH% = 85.4–96.4%, ABTS% = 66.5–93.6%, LOX = 8.7–32.7 μM) when compared to that of the corresponding zinc–mefenamato complexes (RA% = 16.7–41.6%, •OH% = 83–98.5%, ABTS% = 74–94.5%, LOX = 22.9–51.9 μM) recently reported [12]. Furthermore, complexes **1**–**6** can be considered significantly active when compared to other Zn complexes reported in the literature [56,57].

2.4. Interaction with serum albumins

Serum albumins (SAs) are the most abundant proteins in plasma and have the vital role to transport metal ions, drugs and their metal complexes through the blood stream [31]. It is important to examine the interaction of potential drugs with SA since differentiated biological properties of the drug or novel transport pathways may arise. The solutions of human serum albumin (HSA, bearing one tryptophan, Trp-214) and its extensively studied homologue bovine serum albumin (BSA, with two tryptophans, Trp-134 and Trp-212) exhibit an intense fluorescence emission when excited at 295 nm, with $\lambda_{em,max}$ = 351 nm and 343 nm, respectively [59]. Complex **1** in buffer solution exhibits a maximum emission at ~330 nm under the same experimental conditions (as also previously reported the Co(II)-tolfenamato and Zn(II)-tolfenamato complexes **2**–**6**) [24,30] and the SA fluorescence spectra have been corrected before the experimental data processing.

The quenching observed in the fluorescence emission spectra of SA solutions upon addition of complex **1** (Fig. 5) may be attributed to changes in protein conformation, subunit association, substrate

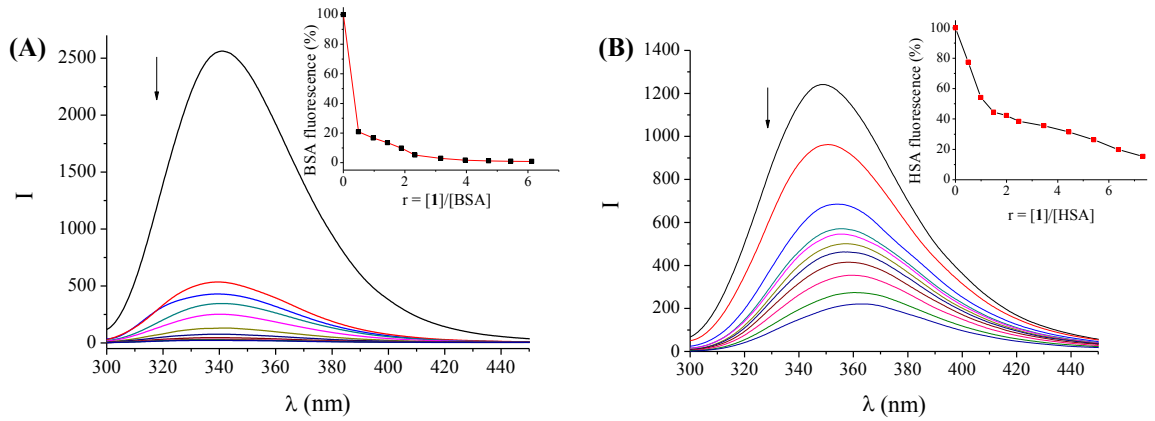

Fig. 5. Emission spectra (λ_{exit} = 295 nm) for (A) BSA ([BSA] = 3 μM) and (B) HSA ([HSA] = 3 μM) in buffer solution (150 mM NaCl and 15 mM trisodium citrate at pH 7.0) in the absence and presence of increasing amounts of complex **1** (up to the value of r = 7.3). The arrow shows the changes of intensity upon increasing amounts of **1**. Insets: Plot of % relative fluorescence intensity at (A) λ_{em} = 342 nm (%) vs r (r = [complex]/[BSA]) for **1** (1% of the initial fluorescence intensity) and (B) λ_{em} = 351 nm (%) vs r (r = [complex]/[HSA]) for **1** (15% of the initial fluorescence intensity).

binding or denaturation [60]. The fluorescence quenching provoked by complex **1** to the BSA fluorescence signal at 342 nm as well as to the HSA fluorescence maximum at 351 nm is significant (Insets in Fig. 5) and is due to possible changes in protein secondary structure leading to changes in tryptophan environment of SA, and thus indicating the binding of the complex to SA [61].

The Stern–Volmer and Scatchard graphs may be used in order to study the interaction of a quencher with serum albumins. The values (Table 2) of the quenching constant, k_q (in M^{-1} s^{-1}), as calculated by the Stern–Volmer equation (Eq. S(1)) [60] and plots (data not shown), are higher ($>10^{13}$ M^{-1} s^{-1}) than diverse kinds of quenchers for biopolymers fluorescence (2×10^{10} M^{-1} s^{-1}) indicating the existence of static quenching mechanism [60]. These values indicate good SA quenching ability and the k_q values of the complex are higher than the corresponding values of free Htolf. Furthermore, complex **1** exhibits the highest quenching ability for BSA (k_q = 7.07(±0.07) × 10^{14} M^{-1} s^{-1}) among Zn-tolfenamato complexes **1**–**6** [24].

The values of the association binding constant, K (in M^{-1}), and the number of binding sites per albumin, n, for complex **1** have been obtained from the corresponding Scatchard equation (Eq. S(3)) [60] and plots (data not shown) and are cited in Table 2. It is obvious that complex **1** exhibits higher K and n values than free Htolf; indeed, complex **1** presents the highest SA binding constants among Zn(II)-tolfenamato complexes **1**–**6** [24]. Comparing the affinity of complex **1** for BSA and HSA (K values), it is obvious that it shows higher affinity for BSA than HSA.

Table 2
The BSA and HSA binding constants and parameters (K_{sv}, k_q, K, n) derived for the Htolf and complexes **1**–**6**.

Compound	k_q (M^{-1} s^{-1})	K (M^{-1})	n
BSA			
Htolf [30]	2.18(±0.12) × 10^{13}	1.60 × 10^5	1.11
$[Zn(tolf)_2(Hpko)_2]$, **1**	7.07(±0.07) × 10^{14}	2.40 × 10^6	1.01
[Zn(tolf)(phen)Cl], **2** [24]	9.99(±0.60) × 10^{13}	5.70 × 10^4	2.09
[Zn(tolf)(bipy)Cl], **3** [24]	1.15(±0.04) × 10^{13}	1.81 × 10^5	0.84
$[Zn(tolf)_2(phen)]$, **4** [24]	1.00(±0.01) × 10^{14}	1.88 × 10^5	1.31
$[Zn(tolf)_2(bipy)]$, **5** [24]	3.67(±0.15) × 10^{13}	6.20 × 10^4	1.70
$[Zn_3(tolf)_6(CH_3OH)_2]$, **6** [24]	1.87(±0.06) × 10^{14}	2.07 × 10^5	1.44
HSA			
Htolf [30]	0.61(±0.04) × 10^{13}	3.12 × 10^5	0.63
$[Zn(tolf)_2(Hpko)_2]$, **1**	1.81(±0.14) × 10^{13}	4.74 × 10^5	0.79
[Zn(tolf)(phen)Cl], **2** [24]	1.41(±0.07) × 10^{13}	4.37 × 10^5	0.65
[Zn(tolf)(bipy)Cl], **3** [24]	0.86(±0.03) × 10^{13}	1.43 × 10^5	0.86
$[Zn(tolf)_2(phen)]$, **4** [24]	4.27(±0.28) × 10^{13}	1.36 × 10^5	1.20
$[Zn(tolf)_2(bipy)]$, **5** [24]	2.84(±0.12) × 10^{13}	1.49 × 10^5	1.16
$[Zn_3(tolf)_6(CH_3OH)_2]$, **6** [24]	1.39(±0.05) × 10^{13}	4.12 × 10^5	0.79

In general, the binding constant of a compound to a protein such as serum albumin should be high enough to allow its binding and possible transfer but also not too high so that it can get released upon arrival at its target. The K values of all complexes **1**–**6** are within such an optimum range; high enough (6.20 × 10^4–2.40 × 10^6 M^{-1}) to allow the binding of the complexes to SAs and also quite below the value of $K \approx 10^{15}$ M^{-1}, which is the association constant of the one of strongest known non-covalent bonds for the interaction between avidin and ligands, suggesting a possible release from the serum albumin to the target cells [61].

In relation to previously reported Co(II) tolfenamato complexes [30], the quenching constants (k_q) and binding constants (K) for complexes **1**–**6** are more pronounced than for their Co(II) analogues for both albumins.

2.5. Interaction with calf-thymus DNA

Metal complexes can bind to double-stranded DNA via covalent and/or noncovalent interactions; upon covalent binding, the replacement of a labile ligand of the complex by a nitrogen base of DNA occurs, while the noncovalent DNA interactions include intercalative (via $\pi \rightarrow \pi^*$ stacking interaction of the complex and DNA nucleobases), external electrostatic (as a result of Coulomb forces of metal complexes and the phosphate groups of DNA) and groove (through van der Waals interaction or hydrogen-bonding or hydrophobic bonding along major or minor groove of DNA helix) binding of metal complexes inside the DNA helix, along major or minor groove [12,30,45,46,62]. The possibility of the existence of anticancer and/or anti-inflammatory activity of the NSAIDs and their complexes could be also related to their ability to bind to DNA [19,20]; within this context, DNA-binding studies should be of significant interest, although the number of such studies involving NSAIDs and their complexes so far is rather limited; e.g. complexes of oxicam NSAIDs bind to DNA via intercalation [20] and the interaction of DNA with a series of zinc(II), cobalt(II) and copper(II) complexes of NSAIDs complexes has been studied and reported quite recently [12,21,30,45,46].

2.5.1. Study of the DNA-binding with UV spectroscopy

The changes observed in the UV spectra upon titration may provide evidence of the existing interaction mode, since a

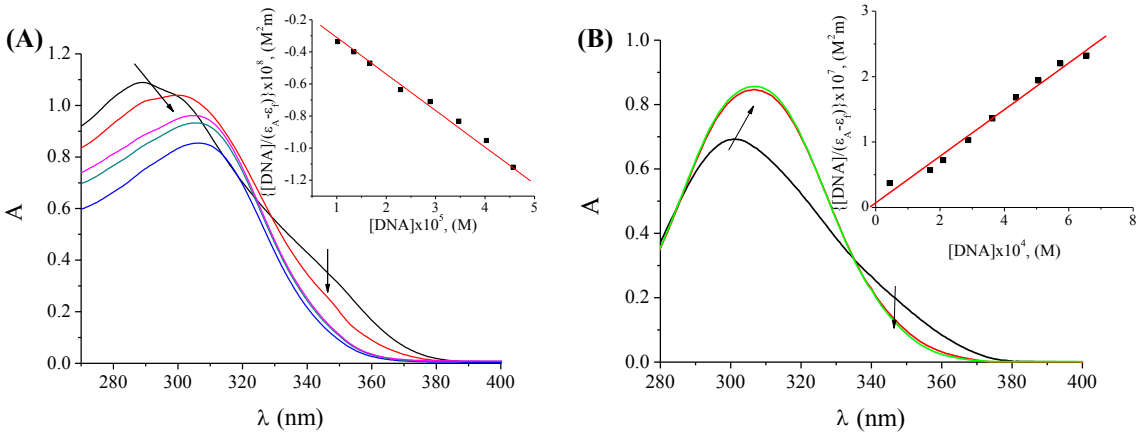

Fig. 6. UV spectra of DMSO solution (1×10^{-5} M) of (A) [Zn(tolf)$_2$(Hpko)$_2$], **1** and (B) [Zn$_3$(tolf)$_6$(CH$_3$OH)$_2$], **6** in the presence of increasing amounts of CT DNA. The arrows show the changes upon increasing amounts of CT DNA. Insets: plot of $[DNA]/(\varepsilon_A - \varepsilon_f)$ vs [DNA].

hypochromism due to $\pi \rightarrow \pi^*$ stacking interactions may appear in the case of the intercalative binding mode, while red-shift (bathochromism) is an evidence of stabilization of the DNA duplex [63]. The UV spectra of a CT DNA solution have been recorded for a constant CT DNA concentration (1.4×10^{-4}–1.6×10^{-4} M) in different [complex]/[DNA] mixing ratios (r) (complex = **1**–**6**) (up to $r = 0.3$). UV spectra of CT DNA in the presence of complex **6** derived for diverse r values are shown as an example in Fig. S1. The predominant features observed upon the addition of the complexes is the decrease of the intensity at $\lambda_{max} = 258$ nm and a red-shift of the λ_{max} up to 266 nm for all complexes, indicating that the interaction with CT DNA results in the direct formation of a new complex with double-helical CT DNA [64]. The observed hypochromism may be attributed to $\pi \rightarrow \pi^*$ stacking interaction between the aromatic chromophore (either from tolfenamato and/or the N-donor ligands) of the complexes and DNA base pairs consistent with the intercalative binding mode, while the red-shift is an evidence of the stabilization of the CT DNA duplex [12,30,45,46,62].

In the UV spectra of the complexes, the intense absorption bands observed are attributed to the intraligand transitions of the coordinated groups of tolfenamato ligands. Any interaction between each complex and CT DNA could perturb the intra-ligand transitions during the titration upon addition of CT DNA in diverse r values. In general, the changes observed in the UV spectra upon titration may give evidence of the existing interaction mode, since a hypochromism due to $\pi \rightarrow \pi^*$ stacking interactions may appear in the case of the intercalative binding mode, while red-shift (bathochromism) may be observed when the DNA duplex is stabilized.

In the UV spectra of **1**, the band centred at 290 nm (band I) presents a hypochromism of 20% accompanied by a red-shift of 16 nm (up to 306 nm) and the band at 341 nm (band II) exhibits a significant hypochromism of 50% (Fig. 6(A)) resulting in an elimination of the band. These predominant spectra features may suggest tight binding to CT DNA probably by intercalation and stabilization. In the UV spectrum of **6**, the band at 297 nm (band I) presents a hyperchromism of up to 15% accompanied by a red-shift of 11 nm (up to 308 nm), suggesting tight binding and stabilization. Additionally, the band centred at 346 nm (band II) exhibits a significant hypochromism of 30% (Fig. 6(B)) suggesting tight binding to CT DNA probably by intercalation. Further addition of DNA results in a blue-shift with a gradual elimination of this band. A distinct isosbestic point at 334 nm appears upon addition of CT DNA. The behavior of Htolf and complexes **2**–**5** upon addition of CT DNA is quite similar to **6**; the hypochromism of band I varies from 15% for **2** up to 60% for Htolf and the observed hyperchromism of band II is between 9% for **5** and 40% for Htolf (Table 3).

In any case, the exact mode of DNA-binding cannot be merely concluded by UV spectroscopic titration studies and the results collected from the UV titration experiments suggest that all compounds can bind to CT DNA. The observed hypochromic effect for all complexes could be considered evidence of tight binding to CT DNA probably by intercalation; nevertheless, further experiments are necessary to carry out in order to clarify the binding mode and possibly verify the existence of intercalation [65].

The magnitude of the binding strength of complexes with CT DNA may be estimated through the binding constant K_b, which can be obtained by the Wolfe–Shimer equation (Eq. S(4)) [66] and plots $[DNA]/(\varepsilon_A - \varepsilon_f)$ versus [DNA] (e.g. insets in Fig. 6). The K_b values calculated for Htolf and complexes **1**–**6** (Table 3) are relatively high and in most cases are higher than that of free tolfenamic acid suggesting that its coordination to Zn(II) results in a increase of the K_b value. The K_b values suggest a strong binding of the complexes to CT DNA, with complex **1** having the highest K_b value

Table 3
The DNA binding constants (K_b) of Htolf and complexes **1**–**6**.

Compound	Band I (290–297 nm) % of hyperchromism or hypochromism	Band II (346 nm) % of hypochromism	K_b (M^{-1})
Htolf [30]	Hyperchromism, 40%	60%	$5.00(\pm0.10) \times 10^4$
[Zn(tolf)$_2$(Hpko)$_2$], **1**	Hypochromism, 20%	50%	$2.80(\pm0.18) \times 10^5$
[Zn(tolf)(phen)Cl], **2**	Hyperchromism, 20%	15%	$9.30(\pm0.20) \times 10^4$
[Zn(tolf)(bipy)Cl], **3**	Hyperchromism, 10%	30%	$3.56(\pm0.11) \times 10^4$
[Zn(tolf)$_2$(phen)], **4**	Hyperchromism, 10%	18%	$1.77(\pm0.09) \times 10^5$
[Zn(tolf)$_2$(bipy)], **5**	Hyperchromism, 9%	25%	$2.36(\pm0.11) \times 10^4$
[Zn$_3$(tolf)$_6$(CH$_3$OH)$_2$], **6**	Hyperchromism, 15%	30%	$5.26(\pm0.13) \times 10^4$

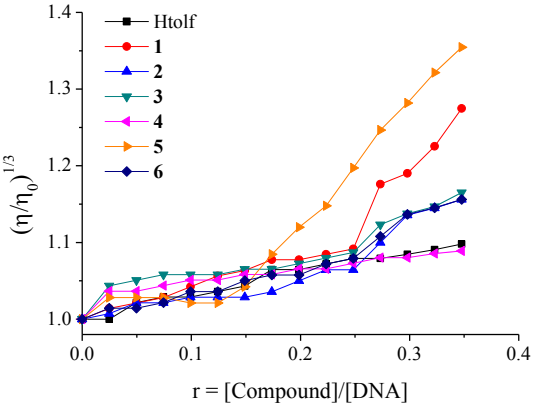

Fig. 7. Relative viscosity of CT DNA $(\eta/\eta_o)^{1/3}$ in buffer solution (150 mM NaCl and 15 mM trisodium citrate at pH 7.0) in the presence of Htolf and complexes **1**–**6** at increasing amounts vs r (r = [Compound]/[DNA]).

(=2.80(±0.18) × 10^5 M^{-1}) among the compounds, and close to that of the classical intercalator EB (=1.23(±0.07) × 10^5 M^{-1}) as calculated in Ref. [67]. The K_b values of complexes **1**–**6** are slightly lower than the corresponding Co(II)-tolfenamato [30] and Zn(II)-mefenamato [12] complexes.

2.5.2. DNA-binding study with viscosity measurements

The information derived by the measurement of the viscosity of DNA solution upon addition of a compound is useful in an attempt to clarify the interaction mode of a compound with DNA, since it is sensitive to DNA length changes; the relation between relative solution viscosity (η/η_0) and DNA length (L/L_0) is given by the equation $L/L_0 = (\eta/\eta_0)^{1/3}$, where L_0 denotes the apparent molecular length in the absence of the compound [12,21,30,45,46,62]. When a compound binds to DNA grooves via a partial or non-classic intercalation (i.e. electrostatic interaction or external groove-binding), a bend or kink in the DNA helix may be provoked resulting in a slight shortening of the effective length of DNA; in such a case, the viscosity of DNA solution shows a slight decrease or remains unchanged [12,21,30,45,46,68] In the case of classic intercalation, the insertion of the compound in between the DNA base pairs with a subsequent increase in the separation of base pairs at intercalation sites and subsequently its hosting results in an increase of the length of the DNA helix leading to an increase of DNA viscosity, the magnitude of which is in accordance to the strength of the interaction.

Viscosity measurements were carried out on CT DNA solutions (0.1 mM) upon addition of increasing amounts of Htolf or complexes **1**–**6** (up to the value of r = 0.35). The addition of the compounds results in a moderate or significant (for **1** and **5**) increase in the relative viscosity of DNA (Fig. 7). This may be explained by the insertion of the complexes in between the DNA base pairs, leading to an increase in the separation of base pairs at intercalation sites and, thus, an increase in overall DNA length. In conclusion, the observed increase of the DNA viscosity in the presence of increasing amounts of the complexes may be considered as an evidence of the existence of an intercalative binding mode to DNA; a conclusion which completely enforces the preliminary findings from UV spectroscopic studies.

2.5.3. Competitive study with ethidium bromide

The intercalation of ethidium bromide (EB = 3,8-diamino-5-ethyl-6-phenyl-phenanthridinium bromide) to CT DNA occurs via the insertion of the planar EB phenanthridine ring in between adjacent base pairs on the DNA double helix. This intercalation results in the appearance of intense fluorescence emission which is due to the formation of the EB-DNA complex. Thus, EB is considered a typical indicator of intercalation since upon the addition of a compound, capable to act as a DNA-intercalator equally or more strongly than EB, into a solution of the EB-DNA compound, a quenching of the DNA-induced EB fluorescence emission may appear [69]. Htolf and complexes **1**–**6** do not show any significant fluorescence at room temperature in solution or in the presence of CT DNA, when excited at 540 nm. Furthermore, the addition of the compounds to a solution containing EB does not provoke quenching of free EB fluorescence and new peaks do not appear in the spectra. Within this context, the changes observed in the fluorescence emission spectra of a solution containing the EB-DNA compound upon addition of the complexes can be used to study the ability of the compounds to displace EB from the EB-DNA complex. The emission spectra of pre-treated EB-CT DNA in the absence and presence of each complex have been recorded for [EB] = 20 μM and [DNA] = 26 μM for increasing amounts of the complex up to the value of r = 0.05 (Fig. 8(A)). The addition of complexes **1**–**6** at diverse r values results in a significant decrease of the intensity of the emission band of the DNA-EB system at 592 nm (the final fluorescence is up to 18–32% of the initial EB-DNA fluorescence intensity in the presence of the complexes) indicating the competition of the complexes with EB in binding to DNA (Fig. 8(B)). The observed quenching of DNA-EB fluorescence by the complexes suggests that the complexes have significant ability to displace EB from the DNA-EB compound, thus

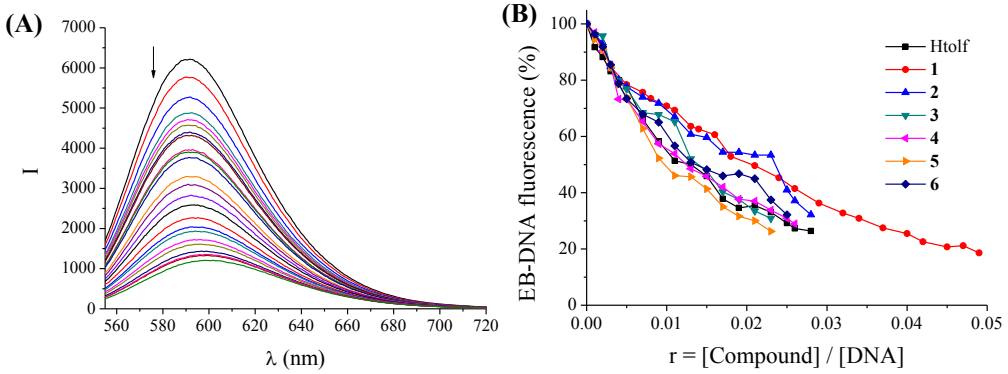

Fig. 8. (A) Fluorescence emission spectra (λ_{exit} = 540 nm) for EB-DNA ([EB] = 20 μM, [DNA] = 26 μM) in buffer solution in the absence and presence of increasing amounts of complex **1** (up to the value of r = 0.05). The arrow shows the changes of intensity upon increasing amounts of **1**. (B) Plot of EB relative fluorescence emission intensity at λ_{em} = 592 nm (%) vs r (r = [complex]/[DNA]) in the presence of Htolf and complexes **1**–**6** (up to 26% of the initial EB-DNA fluorescence intensity for Htolf, 19% for **1**, 32% for **2**, 31% for **3**, 29% for **4**, 26% for **5** and 32% for **6**).

Table 4
Percentage of EB-DNA fluorescence emission quenching (Δ*I*/*I*o, %) and Stern–Volmer constants (K_{SV}) for Htolf and complexes **1**–**6**.

Compound	EB-DNA fluorescence quenching (%)	K_{sv} (M^{-1})
Htolf [30]	74	$1.15(\pm0.04) \times 10^6$
$[Zn(tolf)_2(Hpko)_2]$, **1**	81	$1.15(\pm0.06) \times 10^6$
[Zn(tolf)(phen)Cl], **2**	68	$5.04(\pm0.18) \times 10^5$
[Zn(tolf)(bipy)Cl], **3**	69	$1.11(\pm0.05) \times 10^6$
$[Zn(tolf)_2(phen)]$, **4**	71	$1.04(\pm0.02) \times 10^6$
$[Zn(tolf)_2(bipy)]$, **5**	74	$1.38(\pm0.05) \times 10^6$
$[Zn_3(tolf)_6(CH_3OH)_2]$, **6**	68	$8.44(\pm0.22) \times 10^5$

subsequently interacting with CT DNA by the intercalative mode [12,21,30,45,46,62].

The Stern–Volmer constant, K_{SV}, is used to evaluate the quenching efficiency for each compound according to the Stern–Volmer equation (Eq. S(5)) and is obtained from the diagram Io/I vs [Q]. The Stern–Volmer plots of DNA-EB for the compounds (e.g. for complex **1** in Fig. S2) illustrate that the quenching of EB bound to DNA by the compounds is in good agreement ($R = 0.99$) with the linear Stern–Volmer equation (Eq. (S5)), which proves that the replacement of EB bound to DNA by each compound results in a decrease in the fluorescence intensity [32,33,46,47,50]. The obtained values of K_{SV} (Table 4) are high and show that the complexes can bind tightly to DNA with complex **5** exhibiting the highest K_{sv} value ($=1.38(\pm0.05) \times 10^6$ M^{-1}) among the complexes. The K_{sv} values of complexes **1**–**6** are lower than those of Zn(II)-mefenamato complexes [12] and of the same magnitude to their Co(II)-tolfenamato analogues [30].

3. Conclusions

The synthesis and characterization of the neutral zinc(II) complex with the non-steroidal anti-inflammatory drug tolfenamic acid in the presence of the nitrogen-donor heterocyclic ligand 2,2′-dipyridylketone oxime has been achieved. The crystal structure of the complex $[Zn(tolf)_2(Hpko)_2]$ has been determined by X-ray crystallography revealing the coordination of the deprotonated monodentate tolfenamato ligands to zinc atom via a carboxylato oxygen and of neutral bidentate Hpko ligands via the ketoxime nitrogen and a pyridyl nitrogen.

Complex **1** shows high quenching ability of the BSA and HSA fluorescence and tight binding affinity to these proteins providing relatively high binding constants which are in the optimum range to allow the binding, the transfer and the release upon arrival at the targets. Complex **1** exhibits higher SA-binding constants than a series previously reported Zn(II)-tolfenamato complexes **2**–**6**.

All Zn(II)-tolfenamato complexes **1**–**6** have been tested *in vitro* for their free radical scavenging activity and inhibitory activity on soybean lipoxygenase and were found to be more active than free tolfenamic acid. All complexes exhibit low to moderate DPPH radical scavenging activity and significantly high scavenging activity against hydroxyl and superoxide radicals; they also present significant inhibition against soybean lipoxygenase. Complex $[Zn(tolf)_2(phen)]$, **4** is the most active scavenger of all radicals tested and the most potent LOX inhibitor.

UV spectroscopic titration studies and viscosity measurements have revealed the ability of complexes **1**–**6** to bind to CT DNA. The binding strength of the complexes with CT DNA calculated with UV spectroscopic titrations have shown that **1** exhibits the highest K_b ($K_b = 2.80(\pm0.18) \times 10^5$ M^{-1}) value among the complexes examined, which is of the same order to the K_b value of EB. Competitive DNA-binding studies with EB have revealed a moderate ability of the complexes to displace the typical intercalator EB from the EB-CT DNA complex indicating intercalation as a possible mode of their interaction with CT DNA. The intercalative binding mode has been also confirmed by viscosity measurements of CT DNA solutions in the presence of the complexes.

The reported albumin binding studies is a first attempt to evaluate the ability of the complexes to bind to serum proteins and such studies could be expanded to more serum proteins. The results of the antioxidant activity of the complexes are promising since the complexes are more active than the reference compounds such as trolox and caffeic acid and the ability of the reported compounds to act as DNA intercalators may open a new window for their use as potential metallodrugs.

4. Experimental

4.1. Materials and instrumentation

Tolfenamic acid, $ZnCl_2$, Hpko, KOH, trisodium citrate, NaCl, CT DNA, BSA, HSA and EB were purchased from Sigma–Aldrich Co and all solvents were purchased from Merck. All the chemicals and solvents were reagent grade and were used as purchased.

DNA stock solution was prepared by dilution of CT DNA to buffer (containing 150 mM NaCl and 15 mM trisodium citrate at pH 7.0) followed by exhaustive stirring at 4 °C for three days, and kept at 4 °C for no longer than a week. The stock solution of CT DNA gave a ratio of UV absorbance at 260 and 280 nm (A_{260}/A_{280}) of 1.85, indicating that the DNA was sufficiently free of protein contamination. The DNA concentration was determined by the UV absorbance at 260 nm after 1:20 dilution using $\varepsilon = 6600$ M^{-1} cm^{-1}.

Infrared (IR) spectra (400–4000 cm^{-1}) were recorded on a Nicolet FT-IR 6700 spectrometer with samples prepared as KBr pellets. UV–visible (UV–vis) spectra were recorded as nujol mulls and in solution at concentrations in the range 10^{-5}–10^{-3} M on a Hitachi U-2001 dual beam spectrophotometer. C, H and N elemental analysis were performed on a Perkin–Elmer 240B elemental analyzer. Molar conductivity measurements were carried out in 1 mM DMSO solution of the complexes with a Crison Basic 30 conductometer. Fluorescence spectra were recorded in solution on a Hitachi F-7000 fluorescence spectrophotometer. Viscosity experiments were carried out using an ALPHA L Fungilab rotational viscometer equipped with an 18 mL LCP spindle.

4.2. Synthesis of complex $[Zn(tolf\text{-}O)_2(Hpko\text{-}N,N')_2]\cdot MeOH$, 1·MeOH

Tolfenamic acid (0.4 mmol, 104 mg) was dissolved in methanol (15 mL) followed by the addition of KOH (0.4 mmol, 22 mg). After 1 h stirring, the resultant solution was added slowly and simultaneously with a methanolic solution of Hpko (0.4 mmol, 80 mg), to a methanolic solution (10 mL) of $ZnCl_2$ (0.2 mmol, 27 mg) and was stirred for 30 min. The solution was left for slow evaporation. Pale yellow crystals of $[Zn(tolf)_2(Hpko)_2]\cdot MeOH$, **4**·MeOH (110 mg, 55%) suitable for X-ray structure determination were deposited after two weeks (found C, 59.87; H, 4.40; N, 10.85; $C_{51}H_{44}Cl_2N_8O_7Zn$ (MW = 1017.21) requires C, 60.22; H, 4.36; N, 11.01%). IR: ν_{max}/cm^{-1}; $\nu_{asym}(CO_2)$: 1584 (vs); $\nu_{sym}(CO_2)$: 1387 (vs); $\Delta = 197$ cm^{-1} (KBr disk); UV–vis: λ/nm (ε/M^{-1} cm^{-1}) as nujol mull: 342(sh), 297(sh); in DMSO: 345(sh) (1600), 302 (11,300). ^1H NMR in DMSO-d_6 (δ/ppm), (numbering of the ligands in Schemes 1 and S1): 2.21 (6H, s, H^{10}-tolf), 6.72 (2H, t (J = 7.5 Hz), H^3-tolf), 6.92 (2H, d ($J = 8.1$ Hz), H^5-tolf), 7.12 (4H, m ($J = 8.0$ Hz), H^8-and H^9-tolf), 7.25 (4H, t ($J = 7.4$ Hz), H^4- and H^7-tolf), 7.40 (4H, t ($J = 6.2$ Hz), H^4- and $H^{4'}$-Hpko), 7.54 (2H, d (J = 7.5 Hz), $H^{6'}$-Hpko), 7.79 (2H, d ($J = 7.0$ Hz), H^6-Hpko), 7.88 (4H, m ($J = 7.5$ Hz), H^5- and $H^{5'}$-Hpko), 7.98 (2H, d ($J = 7.8$ Hz), H^2-tolf), 8.47 (2H, d ($J = 4.0$ Hz), $H^{3'}$-Hpko),

8.62 (2H, d ($J = 4.0$ Hz), H^3-Hpko), 10.20 (2H, s, H^6-tolf), 12.21 (2H, s, H^1-Hpko). The complex is soluble in DMF and DMSO ($\Lambda_M = 13$ μS/cm, 1 mM in DMSO).

4.3. Synthesis of complexes **2**–**6**

The synthesis, the physicochemical and IR spectroscopic data for complexes **2**–**6** have been thoroughly presented in Ref. [24]. Herein the ^{1}H NMR spectral features of the complexes are presented (numbering of the ligands is presented in Schemes 1 and S1).

4.3.1. *[Zn(tolf)(phen)Cl],* ***2***

^{1}H NMR in DMSO-d_6 (δ/ppm): 2.11 (3H, s, H^{10}-tolf), 6.66 (1H, t ($J = 7.1$ Hz), H^3-tolf), 6.89 (1H, d ($J = 8.0$ Hz), H^5-tolf), 7.09 (2H, m ($J = 7.5$ Hz), H^8- and H^9-tolf), 7.20 (2H, m ($J = 6.5$ Hz), H^4- and H^7-tolf), 7.88 (1H, d ($J = 7.6$ Hz), H^2-tolf), 8.06 (2H, m ($J = 6.0$ Hz), H^3- and H^8-phen), 8.24 (2H, s, H^5- and H^6-phen), 8.84 (2H, d ($J = 8.1$ Hz), H^4- and H^7-phen), 9.15 (2H, s, H^2- and H^9-phen), 10.51 (1H, s, H^6-tolf).

4.3.2. *[Zn(tolf)(bipy)Cl],* ***3***

^{1}H NMR in DMSO-d_6 (δ/ppm): 2.19 (3H, s, H^{10}-tolf), 6.71 (1H, t ($J = 7.4$ Hz), H^3-tolf), 6.94 (1H, d ($J = 8.1$ Hz), H^5-tolf), 7.13 (2H, m ($J = 7.1$ Hz), H^8- and H^9-tolf), 7.26 (2H, m ($J = 7.2$ Hz), H^4- and H^7-tolf), 7.63 (2H, t ($J = 6.0$ Hz), H^4- and $H^{4'}$-bipy), 7.94 (1H, d ($J = 6.7$ Hz), H^2-tolf), 8.14 (2H, t ($J = 7.0$ Hz), H^6- and $H^{6'}$-bipy), 8.54 (2H, d ($J = 7.8$ Hz), H^5- and $H^{5'}$-bipy), 8.80 (2H, d ($J = 4.5$ Hz), H^3- and $H^{3'}$-bipy), 10.36 (1H, s, H^6-tolf).

4.3.3. *[Zn(tolf)$_2$(phen)],* ***4***

^{1}H NMR in DMSO-d_6 (δ/ppm): 2.11 (6H, s, H^{10}-tolf), 6.66 (2H, t ($J = 7.2$ Hz), H^3-tolf), 6.89 (2H, d ($J = 8.1$ Hz), H^5-tolf), 7.08 (4H, m ($J = 6.8$ Hz), H^8- and H^9-tolf), 7.20 (4H, m ($J = 8.0$ Hz), H^4- and H^7-tolf), 7.88 (2H, d ($J = 7.1$ Hz), H^2-tolf), 8.06 (2H, m ($J = 6.0$ Hz), H^3- and H^8-phen), 8.24 (2H, s, H^5- and H^6-phen), 8.85 (2H, d ($J = 7.2$ Hz), H^4- and H^7-phen), 9.15 (2H, s, H^2- and H^9-phen), 10.45 (2H, s, H^6-tolf).

4.3.4. *[Zn(tolf)$_2$(bipy)],* ***5***

^{1}H NMR in DMSO-d_6 (δ/ppm): 2.19 (6H, s, H^{10}-tolf), 6.71 (2H, t ($J = 7.3$ Hz), H^3-tolf), 6.92 (2H, d ($J = 8.1$ Hz), H^5-tolf), 7.12 (4H, m ($J = 7.5$ Hz), H^8- and H^9-tolf), 7.25 (4H, m ($J = 6.5$ Hz), H^4- and H^7-tolf), 7.63 (2H, m ($J = 6.5$ Hz), H^4- and $H^{4'}$-bipy), 7.94 (2H, d ($J = 7.7$ Hz), H^2-tolf), 8.13 (2H, t ($J = 6.3$ Hz), H^6- and $H^{6'}$-bipy), 8.54 (2H, d ($J = 7.5$ Hz), H^5- and $H^{5'}$-bipy), 8.80 (2H, d ($J = 4.1$ Hz), H^3- and $H^{3'}$-bipy), 10.36 (2H, s, H^6-tolf).

4.3.5. *[Zn$_3$(tolf)$_6$(MeOH)$_2$],* ***6***

^{1}H NMR in DMSO-d_6 (δ/ppm): 2.24 (18H, s, H^{10}-tolf), 6.74 (6H, m ($J = 7.2$ Hz), H^3-tolf), 6.94 (6H, d ($J = 8.2$ Hz), H^5-tolf), 7.10 (12H, m ($J = 2.2$ Hz), H^8- and H^9-tolf), 7.35 (12H, m ($J = 6.5$ Hz), H^4- and H^7-tolf), 7.97 (6H, d ($J = 7.2$ Hz), H^2-tolf), 10.38 (6H, s, H^6-tolf).

4.4. X-ray crystallography

X-ray diffraction data for **1** were collected on an Oxford Diffraction SuperNova diffractometer with Mo microfocus X-ray source (Kα radiation, $\lambda = 0.71073$ Å) with mirror optics and an Atlas detector. The structure was solved by direct methods implemented in SIR92 [70] and refined by a full-matrix least-squares procedure based on F^2 using SHELXL-97 [71]. All non-hydrogen atoms were refined anisotropically. The hydrogen atoms were placed at calculated positions and treated using appropriate riding models. The programs Mercury [72], and Platon [73] were used for data analysis (Table S5).

5. Biological assays

5.1. Antioxidant biological assay

In the *in vitro* assays each experiment was performed at least in triplicate and the standard deviation of absorbance was less than 10% of the mean.

5.1.1. *Determination of the reducing activity of the stable radical DPPH*

To a solution of DPPH (0.1 mM) in absolute ethanol an equal volume of the compounds dissolved in ethanol was added. Ethanol was used as control solution. The concentration of the solution of the compounds was 0.1 mM. The absorbance at 517 nm was recorded at room temperature, after 20 and 60 min in order to examine the time-dependence of the radical scavenging activity [45,46]. The radical scavenging activity of the compounds was expressed as the percentage reduction of the absorbance values of the initial DPPH solution (RA%). NDGA and BHT were used as reference compounds.

5.1.2. *Competition of the tested compounds with DMSO for hydroxyl radicals*

The hydroxyl radicals generated by the Fe^{3+}/ascorbic acid system, were detected according to Nash [45,46], by the determination of formaldehyde produced from the oxidation of DMSO. The reaction mixture contained EDTA (0.1 mM), Fe^{3+} (167 μM), DMSO (33 mM) in phosphate buffer (50 mM, pH 7.4), the tested compounds (0.1 mM) and ascorbic acid (10 mM). After 30 min of incubation (37 °C) the reaction was stopped with CCl_3COOH (17% w/v) and the absorbance at $\lambda = 412$ nm was measured. Trolox was used as an appropriate standard. The competition of the compounds with DMSO for •OH, generated by the Fe^{3+}/ascorbic acid system, expressed as percent inhibition of formaldehyde production, was used for the evaluation of their hydroxyl radical scavenging activity (•OH%).

5.1.3. *Assay of radical cation scavenging activity*

ABTS was dissolved in water to a 2 mM concentration. ABTS radical cation ($ABTS^{+}$•) was produced by reacting ABTS stock solution with 0.17 mM potassium persulfate and allowing the mixture to stand in the dark at room temperature for 12–16 h before use. Because ABTS and potassium persulfate react stoichiometrically at a ratio of 1:0.5, this will result in incomplete oxidation of the ABTS. Oxidation of the ABTS commenced immediately, but the absorbance was not maximal and stable until more than 6 h had elapsed. The radical was stable in this form for more than 2 days when stored in the dark at room temperature. The $ABTS^{+}$• solution was diluted with ethanol to an absorbance of 0.70 at 734 nm. After addition of 10 μL of diluted compounds or standards (0.1 mM) in DMSO, the absorbance reading was taken exactly 1 min after initial mixing [74]. The radical scavenging activity of the complexes was expressed as the percentage inhibition of the absorbance of the initial ABTS solution (ABTS%). Trolox was used as an appropriate standard.

5.1.4. *Soybean lipoxygenase inhibition study in vitro*

The *in vitro* study was evaluated as reported in Ref. [45]. The tested compounds dissolved in ethanol were incubated at room temperature with sodium linoleate (0.1 mM) and 0.2 mL of enzyme solution ($1/9 \times 10^{-4}$ w/v in saline). The conversion of sodium linoleate to 13-hydroperoxylinoleic acid at 234 nm was recorded and compared with the appropriate standard inhibitor caffeic acid.

5.2. Albumin binding experiments

The protein binding study was performed by tryptophan fluorescence emission quenching experiments using bovine (BSA, 3 μM) or human serum albumin (HSA, 3 μM) in buffer (containing 15 mM trisodium citrate and 150 mM NaCl at pH 7.0). The quenching of the emission intensity of tryptophan residues of BSA at 342 nm or HSA at 351 nm was monitored using complex **1** as quencher with increasing concentration since **1** in buffer solutions does not exhibit any emission spectra under the same experimental conditions [46,47]. Fluorescence spectra were recorded from 300 to 500 nm at an excitation wavelength of 295 nm. The Stern–Volmer (Eq. S(1)) and Scatchard equations (Eq. S(3)) and graphs have been used in order to study the interaction of each quencher with serum albumins.

5.3. DNA binding studies

The interaction of complexes **1**–**6** with CT DNA has been studied with UV spectroscopy in order to investigate the possible binding modes to CT DNA and to calculate the binding constants to CT DNA (K_b). In UV titration experiments, the spectra of CT DNA in the presence of each compound have been recorded for a constant CT DNA concentration in diverse [compound]/[CT DNA] mixing ratios (r). The binding constants, K_b, of the compounds with CT DNA have been determined using the UV spectra of the compound recorded for a constant concentration in the absence or presence of CT DNA for diverse r values. Control experiments with DMSO were performed and no changes in the spectra of CT DNA were observed.

Viscosity experiments were carried out using an ALPHA L Fungilab rotational viscometer equipped with an 18 mL LCP spindle and the measurements were performed at 100 rpm. The viscosity of a DNA solution has been measured in the presence of increasing amounts of complexes **1**–**6**. The obtained data are presented as $(\eta/\eta_0)^{1/3}$ versus r, where η is the viscosity of DNA in the presence of complex, and η_0 is the viscosity of DNA alone in buffer solution.

The competitive studies of each compound with EB have been investigated with fluorescence spectroscopy in order to examine whether the compound can displace EB from its CT DNA-EB complex. The CT DNA-EB complex was prepared by adding 20 μM EB and 26 μM CT DNA in buffer (150 mM NaCl and 15 mM trisodium citrate at pH 7.0). The intercalating effect of complexes **1**–**6** with the DNA-EB complex was studied by adding a certain amount of a solution of the compound step by step into the solution of the DNA-EB complex. The influence of the addition of each compound to the DNA-EB complex solution has been obtained by recording the variation of fluorescence emission spectra.

Acknowledgements

This research has been co-financed by European Social Fund (ESF) and Greek National Funds (National Strategic Reference Framework (NSRF): Heracleitus II and Archimides III. Financial support from the Slovenian Research Agency (ARRS) through project P1-0175 is gratefully acknowledged. This project was also supported by EU COST Action CM1105.

Appendix A. Supplementary material

CCDC 910551 contains the supplementary crystallographic data for this paper. These data can be obtained free of charge via www.ccdc.cam.ac.uk/conts/retrieving.html (or from the Cambridge Crystallographic Data Centre, 12 Union Road, Cambridge CB21EZ, UK; fax: +44 1223 336 033).

Appendix B. Supplementary data

Supplementary data related to this article can be found at http://dx.doi.org/10.1016/j.ejmech.2013.12.019.

References

[1] G.K. Walkup, S.C. Burdette, S.J. Lippard, R.Y. Tsien, J. Am. Chem. Soc. 122 (2000) 5644–5645.
[2] L.A. Finney, T.V. O'Halloran, Science 300 (2003) 931–936.
[3] I. Turel, J. Kljun, Curr. Top. Med. Chem. 11 (2011) 2661–2687.
[4] C.P. Larson, U.R. Saha, H. Nazrul, PLoS Med. 6 (2009) e1000175.
[5] E.C. Fusch, B. Lippert, J. Am. Chem. Soc. 116 (1994) 7204–7209.
[6] M. Di Vaira, C. Bazzicalupi, P. Orioli, L. Messori, B. Bruni, P. Zatta, Inorg. Chem. 43 (2004) 3795–3797.
[7] Z. Li, F. Wu, Y. Gong, C. Hu, Y. Zhang, M. Gan, Chin. J. Chem. 25 (2007) 1809–1814.
[8] N.C. Kasuga, K. Sekino, M. Ishikawa, A. Honda, M. Yokoyama, S. Nakano, N. Shimada, C. Koumo, K. Nomiya, J. Inorg. Biochem. 96 (2003) 298–310.
[9] J. d'Angelo, G. Morgant, N.E. Ghermani, D. Desmaele, B. Fraisse, F. Bonhomme, E. Dichi, M. Sghaier, Y. Li, Y. Journaux, J.R.J. Sorenson, Polyhedron 27 (2008) 537–546.
[10] H. Sakurai, Y. Kojima, Y. Yoshikawa, K. Kawabe, H. Yasui, Coord. Chem. Rev. 226 (2002) 187–198.
[11] Q. Zhou, T.W. Hambley, B.J. Kennedy, P.A. Lay, P. Turner, B. Warwick, J.R. Biffin, H.L. Regtop, Inorg. Chem. 39 (2000) 3742–3748.
[12] A. Tarushi, Z. Karaflou, J. Kljun, I. Turel, G. Psomas, A.N. Papadopoulos, D.P. Kessissoglou, J. Inorg. Biochem. 128 (2013) 85–96.
[13] C.P. Duffy, C.J. Elliott, R.A. O'Connor, M.M. Heenan, S. Coyle, I.M. Cleary, K. Kavanagh, S. Verhaegen, C.M. O'Loughlin, R. NicAmhlaoibh, M. Clynes, Eur. J. Cancer 34 (1998) 1250–1259.
[14] A.R. Amin, P. Vyas, M. Attur, J. Leszczynskapiziak, I.R. Patel, G. Weissmann, S.B. Abramson, Proc. Natl. Acad. Sci. 92 (1995) 7926–7930.
[15] K. Kim, J. Yoon, J.K. Kim, S.J. Baek, T.E. Eling, W.J. Lee, J. Ryu, J.G. Lee, J. Lee, J. Yoo, Biochem. Biophys. Res. Commun. 325 (2004) 1298–1303.
[16] D.H. Woo, I. Han, G. Jung, Life Sci. 75 (2004) 2439–2449.
[17] M.L. Smith, G. Hawcroft, M.A. Hull, Eur. J. Cancer 36 (2000) 664–674.
[18] A. Inoue, S. Muranaka, H. Fujita, T. Kanno, H. Tamai, K. Utsumi, Free Radical Biol. Med. 37 (2004) 1290–1299.
[19] T. Zhang, T. Otevrel, Z.Q. Gao, Z.P. Gao, S.M. Ehrlich, J.Z. Fields, B.M. Boman, Cancer Res. 61 (2001) 8664–8667.
[20] S. Roy, R. Banerjee, M. Sarkar, J. Inorg. Biochem. 100 (2006) 1320–1331.
[21] G. Psomas, D.P. Kessissoglou, Dalton Trans. 42 (2013) 6252–6276.
[22] P. Lemoine, B. Viossat, N.H. Dung, A. Tomas, G. Morgant, F.T. Greenaway, J.R.J. Sorenson, J. Inorg. Biochem. 98 (2004) 1734–1749.
[23] A. Tarushi, F. Kastanias, V. Psycharis, C.P. Raptopoulou, G. Psomas, D.P. Kessissoglou, Inorg. Chem. 51 (2012) 7460–7462.
[24] A. Tarushi, X. Totta, C. Raptopoulou, V. Psycharis, G. Psomas, D.P. Kessissoglou, Dalton Trans. 41 (2012) 7082–7091.
[25] J.E. Weder, C.T. Dillon, T.W. Hambley, B.J. Kennedy, P.A. Lay, J.R. Biffin, H.L. Regtop, N.M. Davies, Coord. Chem. Rev. 232 (2002) 95–126.
[26] E. Moilanen, H. Kankaanranta, Pharmacol. Toxicol. 75 (Suppl. II) (1994) 60.
[27] D. Kovala-Demertzi, N. Kourkoumelis, A. Koutsodimou, A. Moukarika, E. Horn, E.R.T. Tiekink, J. Organomet. Chem. 620 (2001) 194–201.
[28] D. Kovala-Demertzi, A. Galani, M.A. Demertzis, S. Skoulika, C. Kotoglou, J. Inorg. Biochem. 98 (2004) 358–364.
[29] J. Svorec, S. Lorinc, J. Moncol, M. Melnik, M. Koman, Trans. Met. Chem. 34 (2009) 703–710.
[30] S. Tsiliou, L. Kefala, F. Perdih, I. Turel, D.P. Kessissoglou, G. Psomas, Eur. J. Med. Chem. 48 (2012) 132–142.
[31] C. Tan, J. Liu, H. Li, W. Zheng, S. Shi, L. Chen, L. Ji, J. Inorg. Biochem. 102 (2008) 347–358.
[32] P.C. Andrews, R.L. Ferrero, P.C. Junk, I. Kumar, Q. Luu, K. Nguyen, J.W. Taylor, Dalton Trans. 39 (2010) 2861–2868.
[33] A. Tarushi, J. Kljun, I. Turel, A.A. Pantazaki, G. Psomas, D.P. Kessissoglou, New J. Chem. 37 (2013) 342–355.
[34] A. Tarushi, K. Lafazanis, J. Kljun, I. Turel, A.A. Pantazaki, G. Psomas, D.P. Kessissoglou, J. Inorg. Biochem. 121 (2013) 53–65.
[35] R. Mitra, M.W. Peters, M.J. Scott, Dalton Trans. (2007) 3924–3935.
[36] D.K. Garner, S.B. Fitch, L.H. McAlexander, L.M. Bezold, A.M. Arif, L.M. Berreau, J. Am. Chem. Soc. 124 (2002) 9970–9971.
[37] A. Zianna, G. Psomas, A. Hatzidimitriou, E. Coutouli-Argyropoulou, M. Lalia-Kantouri, J. Inorg. Biochem. 127 (2013) 116–126.
[38] A. Walsh, B. Walsh, B. Murphy, B.J. Hathaway, Acta Crystallogr. B37 (1981) 1512–1520.
[39] X. Chen, Z. Xu, X. Yu, T.C.W. Mak, Polyhedron 13 (1994) 2079–2083.
[40] S. Thirumaran, K. Ramalingama, G. Bocelli, A. Cantoni, Polyhedron 18 (1999) 925–930.
[41] R.A. Coxall, S.G. Harris, D.K. Henderson, S. Parsons, P.A. Tasker, R.E.P. Winpenny, J. Chem. Soc. Dalton Trans. (2000) 2349–2356.
[42] C.J. Milios, T.C. Stamatatos, S.P. Perlepes, Polyhedron 25 (2006) 134–194.
[43] M. Alexiou, I. Tsivikas, C. Dendrinou-Samara, A.A. Pantazaki, P. Trikalitis, N. Lalioti, D.A. Kyriakidis, D.P. Kessissoglou, J. Inorg. Biochem. 93 (2003) 256–264.

[44] R. Cini, G. Giorgi, A. Cinquantini, C. Rossi, M. Sabat, Inorg. Chem. 29 (1990) 5197–5200.
[45] C. Kontogiorgis, D. Hadjipavlou-Litina, J. Enzyme Inhib. Med. Chem. 18 (2003) 63–69.
[46] F. Dimiza, S. Fountoulaki, A.N. Papadopoulos, C.A. Kontogiorgis, V. Tangoulis, C.P. Raptopoulou, V. Psycharis, A. Terzis, D.P. Kessissoglou, G. Psomas, Dalton Trans. 40 (2011) 8555–8568.
[47] F. Dimiza, A.N. Papadopoulos, V. Tangoulis, V. Psycharis, C.P. Raptopoulou, D.P. Kessissoglou, G. Psomas, Dalton Trans. 39 (2010) 4517–4528.
[48] R.N. Young, Eur. J. Med. Chem. 34 (1999) 671–685.
[49] J. Van der Zee, T.E. Eling, R.P. Mason, Biochemistry 28 (1989) 8363–8367.
[50] K.C. Skyrianou, F. Perdih, A.N. Papadopoulos, I. Turel, D.P. Kessissoglou, G. Psomas, J. Inorg. Biochem 105 (2011) 1273–1285.
[51] C. Tolia, A.N. Papadopoulos, C.P. Raptopoulou, V. Psycharis, C. Garino, L. Salassa, G. Psomas, J. Inorg. Biochem 123 (2013) 53–65.
[52] S.B. Bukhari, S. Memona, M.M. Tahir, M.I. Bhanger, J. Mol. Struct. 892 (2008) 39–46.
[53] E. Pontiki, D. Hadjipavlou-Litina, A.T. Chaviara, C.A. Bolos, Bioorg. Med. Chem. Lett. 16 (2006) 2234–2237.
[54] Z. Liu, B. Wang, Z. Yang, Y. Li, D. Qin, T. Li, Eur. J. Med. Chem. 44 (2009) 4477–4484.
[55] P.C. Christidis, Z.D. Georgousis, D. Hadjipavlou-Litina, C.A. Bolos, J. Mol. Struct. 872 (2008) 73–80.
[56] O.A. El-Gammal, G.M. Abu El-Reash, S.E. Ghazy, A.H. Radwan, J. Mol. Struct. 1020 (2012) 6–15.
[57] Y. Li, Z. Yang, Y. Wang, Z. Anorg. Allg. Chem. 637 (2011) 323–330.
[58] E. Pontiki, D. Hadjipavlou-Litina, Bioorg. Med. Chem. 15 (2007) 5819–5827.
[59] J.R. Lakowicz, Principles of Fluorescence Spectroscopy, third ed., Plenum Press, New York, 2006.
[60] Y. Wang, H. Zhang, G. Zhang, W. Tao, S. Tang, J. Luminescence 126 (2007) 211–218.
[61] V. Rajendiran, R. Karthik, M. Palaniandavar, H. Stoeckli-Evans, V.S. Periasamy, M.A. Akbarsha, B.S. Srinag, H. Krishnamurthy, Inorg. Chem. 46 (2007) 8208–8221.
[62] J. Kljun, I. Bratsos, E. Alessio, G. Psomas, U. Repnik, M. Butinar, B. Turk, I. Turel, Inorg. Chem. 52 (2013) 9039–9052.
[63] E.C. Long, J.K. Barton, Acc. Chem. Res. 23 (1990) 271–273.
[64] Q. Zhang, J. Liu, H. Chao, G. Xue, L. Ji, J. Inorg. Biochem. 83 (2001) 49–55.
[65] G. Pratviel, J. Bernadou, B. Meunier, Adv. Inorg. Chem. 45 (1998) 251–262.
[66] A. Wolfe, G. Shimer, T. Meehan, Biochemistry 26 (1987) 6392–6396.
[67] A. Dimitrakopoulou, C. Dendrinou-Samara, A.A. Pantazaki, M. Alexiou, E. Nordlander, D.P. Kessissoglou, J. Inorg. Biochem. 102 (2008) 618–628.
[68] J. Liu, H. Zhang, C. Chen, H. Deng, T. Lu, L. Li, Dalton Trans. (2003) 114–119.
[69] W.D. Wilson, L. Ratmeyer, M. Zhao, L. Strekowski, D. Boykin, Biochemistry 32 (1993) 4098–4104.
[70] A. Altomare, G. Cascarano, C. Giacovazzo, A.C. Guagliardi, M.C. Burla, G. Polidori, M. Camalli, J. Appl. Cryst. 27 (1994) 435.
[71] G.M. Sheldrick, Acta Crystallogr. Sect. A 64 (2008) 112–122.
[72] C.F. Macrae, P.R. Edgington, P. McCabe, E. Pidcock, G.P. Shields, R. Taylor, M. Towler, J. van De Streek, J. Appl. Cryst. 39 (2006) 453–457.
[73] A.L. Spek, Acta Crystallogr. Sect. D. Biol. Crystallogr. 65 (2009) 148–155.
[74] K.R. Prabhakar, V.P. Veerapur, P. Bansal, V. Kumar, M. Reddy, A. Barik, B.K. Reddy, P. Reddanna, K.I. Priyadarsini, M.K. Unnikrishnan, Bioorg. Med. Chem. 14 (2006) 7113–7120.